

# 33 × 33 ARRAYED WAVEGUIDE GRATING MULTIPLEXER USING FLUOROPOLYMER PFS-co-GMA

Hai Ming Zhang,<sup>1</sup> Chun Sheng Ma,<sup>1</sup> Xi Zhen Zhang,<sup>1</sup> Fei Wang,<sup>1</sup> and Da Ming Zhang<sup>1,2</sup>

<sup>1</sup> College of Electronic Science and Engineering  
State Key Laboratory on Integrated Optoelectronics  
Jilin University

Changchun 130012, P.R. China

<sup>2</sup> State Key Laboratory on Applied Optics

Changchun Institute of Optics, Fine Mechanics and Physics  
Chinese Academy of Sciences  
Changchun 130021, P.R. China

Received 31 May 2005

**ABSTRACT:** In this paper, a 33 × 33 arrayed waveguide grating (AWG) multiplexer has been fabricated using the poly(2,3,4,5,6-pentafluorostyrene-co-glycidylmethacrylate) (PFS-co-GMA). The technology process of the device is described, and the measured results are presented. The measured center wavelength is 1550.85 nm, the wavelength channel spacing is about 0.81 nm, and the 3-dB bandwidth is about 0.35 nm. The crosstalk is about -20 dB, and the insertion loss is between 10.4 dB for the central port and 11.9 dB for the edge ports. © 2005 Wiley Periodicals, Inc. *Microwave Opt Technol Lett* 47: 470–472, 2005; Published online in Wiley InterScience (www.interscience.wiley.com). DOI 10.1002/mop.21203

**Key words:** polymer; arrayed waveguide grating; transmission spectrum; insertion loss; crosstalk

## 1. INTRODUCTION

The arrayed waveguide grating (AWG) multiplexer is a key device for wavelength division multiplexing in optical-communication systems [1–4]. Currently, many research groups are devoting themselves to the development of polymer AWG multiplexers, and have fabricated some such devices using various polymeric materials [5]. Polymer AWG multiplexers possess some excellent particular features, including easier fabrication, smaller birefringence [6], and easier control of the refractive index, compared with some other kinds of AWG multiplexers. However, polymer waveguides have higher absorption loss within the range of the 1300–1600-nm communication window, compared with silica-on-silicon waveguides [7]. It is reported that the hydrocarbon bonds (C—H) of polymer increase the intrinsic absorption loss within the wavelength range of 1300–1600 nm. An effective way to reduce the intrinsic absorption loss is to design such polymer materials, in which highly absorbing C—H groups are replaced with very low absorbing fluorocarbon groups (C—F) [7]. Therefore, a fluoropolymer material system with little C—H content is required for fabricating AWG devices.

In this paper, we report the result of a 33 × 33 polymer/Si AWG multiplexer using the poly(2,3,4,5,6-pentafluorostyrene-co-

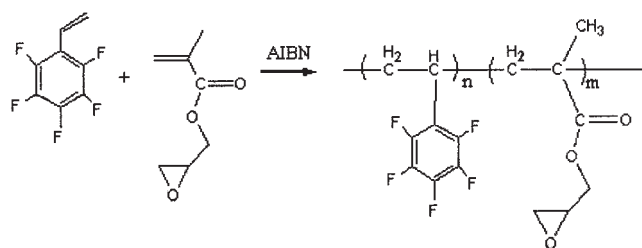


Figure 1 Molecular formula of PFS-co-GMA

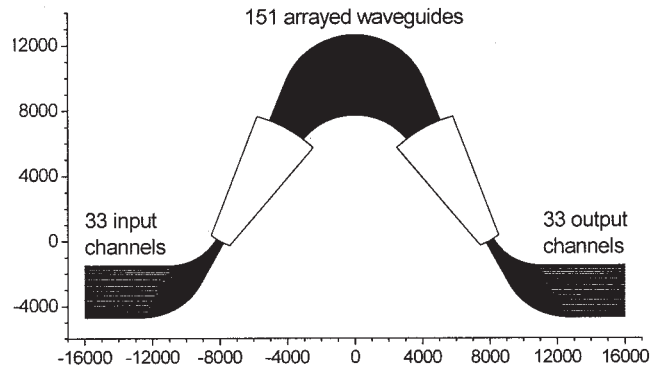


Figure 2 Schematic layout of the designed AWG device

glycidylmethacrylate) (PFS-co-GMA) [8]. In the fabrication, we use the reactive ion etching (RIE) [9] and photolithography. Furthermore, a technique of polishing the waveguide facets is used to ensure minimum coupling loss in the measuring process of the device. The result shows that the measured transmission spectrum of our AWG device is consistent with that in theory.

## 2. FABRICATION AND MEASURED RESULTS

The PFS-co-GMA is chosen as the cladding material, and the styrene (St) is used to regulate the PFS-co-GMA to form the core material with higher refractive index. Figure 1 shows the molecular formula of the material. The core refractive index can be easily controlled from 1.461 to 1.555 through regulating the mol percent of St.

Based on these polymer materials, first we carry out the structural design of the AWG, the schematic waveguide layout of our designed 33 × 33 AWG device is presented in Figure 2, the optimized values of the parameters are listed in Table 1, and the calculated transmission spectrum is plotted in Figure 3, respectively.

In the wavelength range of 1300–1600 nm, the absorption loss of this polymer material predominantly comes from the overtones of the C=O and C—H bond vibrations, whereas those of the C—F show extremely low absorption throughout the above wavelength range [9]. The measured result shows that the extinction coefficient of the material is less than  $5.0 \times 10^{-6}$  in the range of 1500–1600 nm. Therefore, the relative absorption loss is less than 0.4 dB/cm.

As is well known, scattering and process-induced effects can also contribute to the propagation loss of the waveguide. The scattering loss primarily results from dust, bubbles, voids, and cracks. In order to avoid such potential extrinsic sources, it is necessary that all material processes and device-fabrication steps

TABLE 1 Parameters Used in the Design of the Polymer AWG

Central wavelength	$\lambda_0 = 1.550918 \mu\text{m}$
Wavelength spacing	$\Delta\lambda = 0.8 \text{ nm}$
Width and thickness of core	$a = b = 5 \mu\text{m}$
Core refractive index	$n_1 = 1.4704$
Cladding refractive index	$n_2 = 1.463$
Diffraction order	$m = 56$
Pitch of adjacent I/O and arrayed waveguides	$d = 15.5 \mu\text{m}$
Length difference of adjacent arrayed waveguide	$\Delta L = 59.29 \mu\text{m}$
Slab-waveguide focal length	$f = 7838.22 \mu\text{m}$
Free spectral range	FSR = 27.58 nm
Number of I/O channels	$2N + 1 = 33$
Number of arrayed waveguides	$2M + 1 = 151$

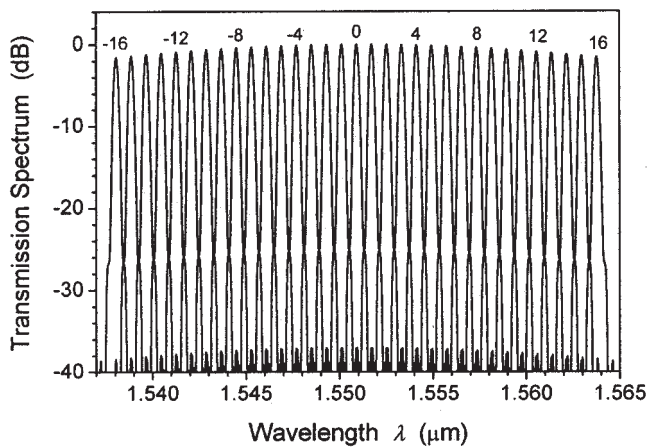


**Figure 3** Calculated transmission spectrum of the designed AWG device for the lossless case

should be performed under traditional clean-room conditions. The process-induced loss mainly results from the sidewall roughness and stress-induced scatterings. For the sake of keeping a minimum sidewall roughness spin-coating and etch-process steps (wet-etching aluminum and RIE) must be performed with great precision. In order to ensure the minimal stress-induced scattering, we spin and coat the undercladding two times and increase its thickness to about 12  $\mu\text{m}$ .

The guide core is buried in the cladding. The fabrication steps are shown in Figure 4 as follows: (a) spin-coating the undercladding and core layers in turn, (b) depositing metal mask, (c) spin-coating photoresist, (d) photolithography, (e) wet etching, (f) RIE, and finally (g) spin-coating the overcladding. Figure 5 shows a scanning electron microscopy (SEM) micrograph of the input channels. The guide core is symmetric and  $5 \times 5 \mu\text{m}^2$  with a core-cladding relative refractive-index difference of 0.5%.

The propagation loss of the waveguide is measured using the following technique. Firstly, we measure the propagation loss to be 5.78 dB for a 5.7-cm-long waveguide at 1550 nm, then we cut it into three parts, of which the lengths are 2.65, 1.83, and 0.78 cm, and their measured propagation losses are 3.83, 3.2, and 2.53 dB, respectively. In order to reduce the coupling loss between the fiber and the waveguide, we polish the facets of the waveguide and

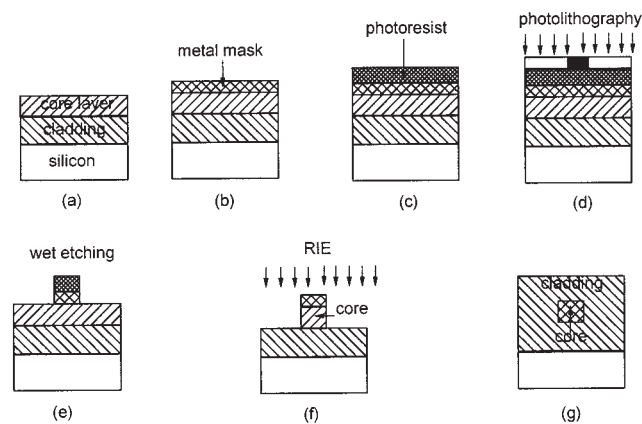


**Figure 4** Process steps of the fabrication of AWG: (a) spin-coating the undercladding and core layers; (b) depositing metal mask; (c) spin-coating photoresist; (d) photolithography; (e) wet-etching; (f) RIE; (g) spin-coating the overcladding

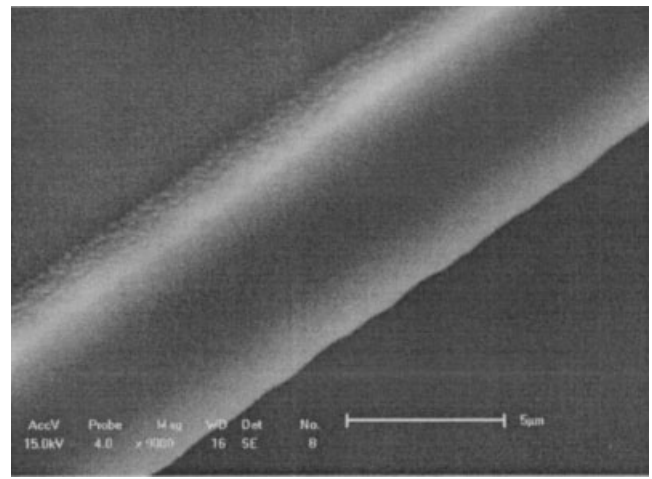


**Figure 5** SEM micrograph of an input channel waveguide after reactive core etching

connect the fiber with the waveguide accurately. The measured data of the propagation loss in Figure 6 show that the propagation loss of the waveguide is about 0.68 dB/cm at 1550 nm.

The spectral-transmission characteristic of the fabricated AWG device is measured using an intelligent test system (IQS-12004B, EXFO). The measured transmission spectrum is presented in Figure 7, where we can see that the crosstalk is about  $-20$  dB, and the insertion loss of our device is between 10.4 dB for the central port and 11.9 dB for the edge ports. Comparing Figure 7 with Figure 3, we find that the shift of the center wavelength between theory and experiment is about 0.07 nm. The measured result shows that the wavelength spacing is about 0.81 nm, and the 3-dB bandwidth is about 0.35 nm. Figure 8 shows a near-field photograph of the demultiplexing spectrum at the output ports of the output channels. Therefore, we can conclude from Figures 7 and 8 that the presented AWG device exhibits good transmission characteristics.

### 3. CONCLUSION

In summary, using the PFS-co-GMA, we have fabricated a  $33 \times 33$  polymer AWG device, of which the variation of the wavelength spacing between the theory and experiment is about 0.07 nm, the

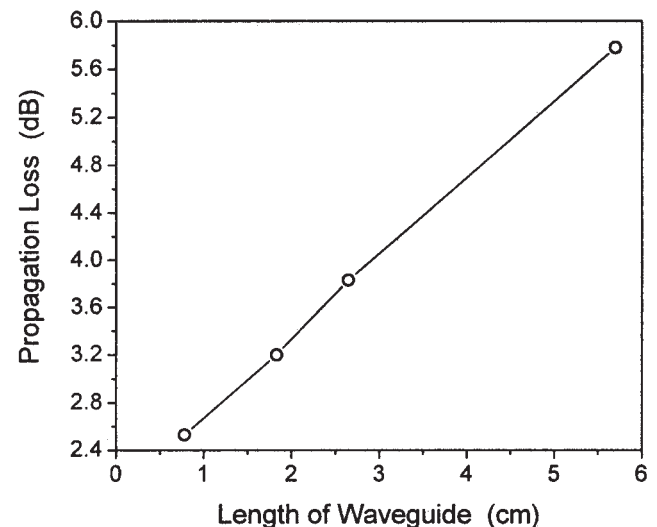


**Figure 6** Measured propagation loss of the waveguide

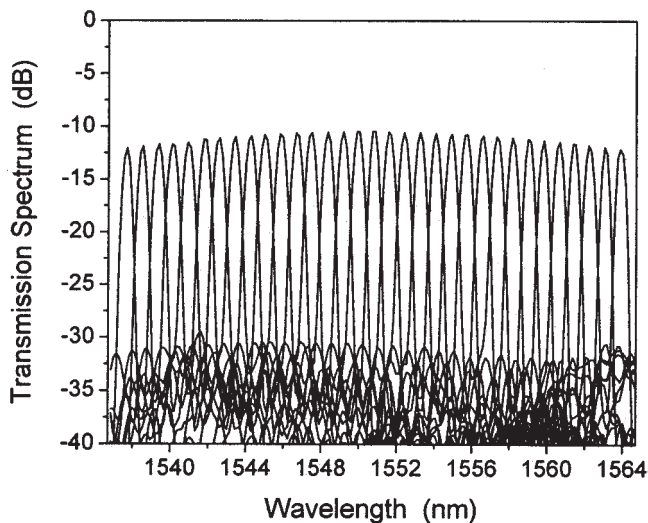


Figure 7 Measured transmission spectrum of the fabricated AWG

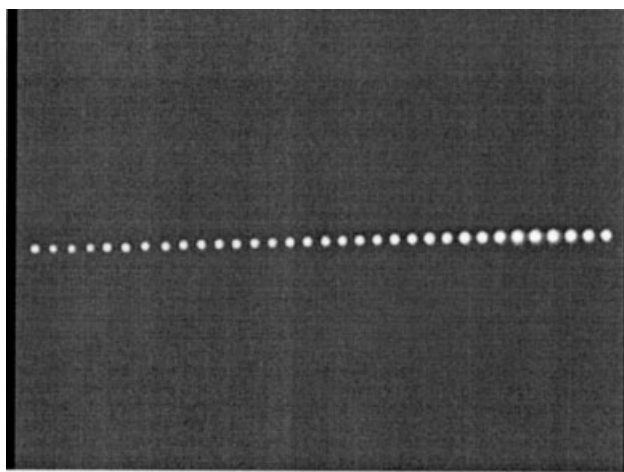


Figure 8 Near-field photograph of the demultiplexing spectrum in the wavelength range of 1536–1564 nm

crosstalk is about  $-20$  dB, and the insertion loss is between 10.4 dB for the central port and 11.9 dB for the edge ports. Currently, we are devoting ourselves to further reducing the loss and crosstalk of the polymer AWG device in order to fabricate this device with better features.

#### ACKNOWLEDGMENT

The authors wish to express their gratitude to the National Science Foundation Council of China (grant no. 60177022), the Science and Technology Council of China (grant nos. G2000036604 and 2001AA312160), and the Changchun Institute of Optics, Fine Mechanics and Physics, Chinese Academy of Sciences (grant no. C03Q14Z) for their generous support of this work.

#### REFERENCES

1. Y.L. Sun, X.Q. Jiang, J.Y. Yang, Y. Tang, and M.H. Wang, Experimental demonstration of two-dimensional multimode-interference optical power splitter, *Chin Phys Lett* 20 (2003), 2182–2184.
2. Z.T. Wang, J.S. Xia, Z.C. Fan, S.W. Chen, and J.Z. Yu, Fabrication of thermo-optic switch in silicon-on-insulator, *Chin Phys Lett* 20 (2003), 2185–2187.
3. X.P. Zheng, Y.L. Chu, W. Zhao, H.Y. Zhang, and Y.L. Guo, Measure-

- ment of root-mean-square phase errors in arrayed waveguide gratings, *Chin Phys Lett* 21 (2004), 335–336.
4. M. Zirngibl, C.H. Joyner, L.W. Stulz, T. Gaiffe, and C. Dragone, Polarization independent waveguide grating multiplexer on InP, *Electron Lett* 29 (1993), 201–202.
5. J. Kobayashi, Y. Inoue, T. Matsuura, and T. Maruno, Tunable and polarization-insensitive arrayed-waveguide grating multiplexer fabricated from fluorinated polyimides, *IEICE Trans Electron E* 81-C (1998), 1020–1026.
6. J. Yang, Q. Zhou, X. Jiang, M. Wang, and R. Chen, Polymer-based electro-optical circular-polarization modulator, *IEEE Photon Technol Lett* 16 (2004), 96–98.
7. A. Yeniay, R.Y. Gao, K. Takayama, R.F. Gao, and F. Garito, Ultra-low-loss polymer waveguides, *J Lightwave Technol* 22 (2004), 154–158.
8. C. Pitois, S. Vukmirovic, A. Hult, D. Wiesmann, and M. Robertsson, Tunable optical add/drop components in silicon-oxynitride waveguide structures, *Macromolecules* 32 (1999), 2903–2909.
9. H. Ma, A.K.Y. Jen, and L.R. Dalton, Polymer-based optical waveguide: Materials, processing, and devices, *Adv Mater* 14 (2002), 1339–1365.

© 2005 Wiley Periodicals, Inc.

## STRONG MICROWAVE SECOND ORDER REJECTION BAND IN OPAL-LIKE STRUCTURES

A. Gastón,<sup>1</sup> M. Beruete,<sup>1</sup> F. Meseguer,<sup>2</sup> M. Sorolla,<sup>1</sup> and J. Sevilla<sup>1</sup>

<sup>1</sup> Electrical and Electronical Engineering Department  
Universidad Pública de Navarra  
31006 Pamplona, Spain

<sup>2</sup> Centro Tecnológico de Ondas  
Unidad Asociada CSIC-UPV  
Universidad Politécnica de Valencia  
46022 Valencia, Spain

Received 30 May 2005

**ABSTRACT:** The electromagnetic-transmission properties of opal-like structures made of glass marbles has been measured. All the cases show strongly rejected bands at frequencies corresponding to a Bragg 2<sup>nd</sup>-order of diffraction. The results show good agreement with appropriate simulations. Moreover, the structure presents a lens effect when placed properly at the output of a conventional horn antenna. © 2005 Wiley Periodicals, Inc. *Microwave Opt Technol Lett* 47: 472–475, 2005; Published online in Wiley InterScience (www.interscience.wiley.com). DOI 10.1002/mop.21204

**Key words:** electromagnetic band gap; macroscopic opal; metamaterials; lens effect

### 1. INTRODUCTION

Periodic patterns of the refraction index have proved to offer very interesting electromagnetic behavior from both the fundamental and the applied points of view. The study of these structures, referred as photonic crystals or electromagnetic band gaps, has generated a huge amount of work and literature [1–5]. Since the first studies in photonic crystals, the ordered piling of dielectric spheres has been one of the structures under study [6]. These materials, which can be found naturally (as the case of opals), can also be fabricated in direct [7, 8] or inverse version (with void spheres surrounded by dielectric) [9]. The work of Yablanovitch and Gmitter [6] stated the impossibility of obtaining a full band gap with opal structures, and stated the index-of-refraction contrast needed to obtain it in the inverse opal structure.